J. Mater. Environ. Sci. 7 (3) (2016) 889-898
ISSN : 2028-2508
CODEN: JMESCN

Theoretical study of Stability and Structure of $Ba^{2+}Ar_n$ (n = 1-25) Clusters

K. Issa[1], K. Abdessalem[1], N. Issaoui[1], S. J. Yaghmour[2], K. Ali[2], B.Oujia[1,2]
[1]*University of Monastir, Sciences Faculty, Department of physics, Tunisia.*
[2]*University of Jeddah, Sciences Faculty, Department of physics, Jeddah.*

Received 27 Feb 2015, Revised 07 Feb 2016, Accepted 16 Feb 2016
**Corresponding author: E-mail: issaoui_noureddine@yahoo.fr*; Tel: (+216-99851543)

Abstract
The structures and stabilities of $Ba^{2+}Ar_n$ (n=25) mixed clusters have been investigated. The stable geometries have been determined by exploring the potential energy surface using the basin-hopping global optimization method. To construct the potential energy surface we have described the $Ba^{2+}Ar$ and Ar-Ar interactions respectively by the Tang and Toennies and Lennard-Jones potentials model. The obtained structures confirm that the barium ion is always solvated in the argon cluster. We have found a bent form (C_{2v}) for $Ba^{2+}Ar_2$ molecule. A pyramidal (C_{3v}) and (C_{4v}) geometries have been found for $Ba^{2+}Ar_3$ and $Ba^{2+}Ar_4$, respectively. A very stable square antiprism (*SA*) structure has been detected for $Ba^{2+}Ar_8$. The $Ba^{2+}Ar_{11}$ cluster has an icosahedron-capped square antiprism structure with Ba^{2+} ion lies between a square and pentagonal ring. For the $Ba^{2+}Ar_{12}$ cluster, we have observed a regular icosahedral geometry indicating the stability of this cluster. The twelve argon atoms complete the first solvation shell around the Ba^{2+} ion. The stable structures of $Ba^{2+}Ar_n$ clusters are based on icosahedral packing. Then, we have obtained the double, triple and quadruple icosahedrons structures for $Ba^{2+}Ar_{18}$, $Ba^{2+}Ar_{22}$ and $Ba^{2+}Ar_{25}$, respectively. We found series of magic numbers n= 8, 9, 10, 12, 18, 19, 22 and 23. Using these data, it will be possible to calculate the excitation cross sections and rates of Ba^{2+} in a collision with Ar atoms.

Keywords: Clusters, Global optimization, Global minimum, Magic numbers, Solvation shell

Introduction
Clusters offer an important opportunity to study and to explain the physical and chemical properties of solvated systems with the solvent size increasing up to the bulk. Van der Waals clusters have received a great attention in the last two decades [1-4]. There is considerable interest in the interactions between metals (neutrals and ions) and ligands. Such interactions are commonplace in the upper atmosphere [5, 6] but also occur in biological processes [7] and are important in industrial applications [8, 9]. Understanding the details of the chemistry is therefore very important in several different fields. The interactions here concern diatomic systems, one metal atom or ion with a single rare gas atom. One might expect the behavior of these complexes to be quite straightforward, with bonding attributable to purely physical interactions, i.e. inductive and Van der Waals forces; however, some unexpected trends have been uncovered and the bonding has proven to be far from simple. The study of molecules or of atoms demounting on rare gas clusters; it can be divided into three main categories [10]; the spectroscopy of the species deposited (generally molecular) by considering that the cluster does not play any role [11-13]. The studies of the aggregate east use like a chemical microreactor making it possible to gather the whole of the reagents [11, 14, 15]. The study of the interaction enters the chromophoric one deposited and the aggregate. These studies can be generally divided into two under-parts: those providing only spectroscopic information such as the absorption spectra, those are generally useful has to know the localization of chromophoric compared to the aggregate [16] and those also providing information on dynamics such as the different output channels, the branching ratios etc. There are also a great number of experimental and theoretical studies studying photo-dissociations of molecules ionized in contact with aggregates of variable size [17-18]. Those make it possible to study the appearing cage effect on the recombination of the species related to electronic relieving according to the number of atoms composing the aggregate.

In the present paper, we investigate the solvation of Ba^{2+} ion in argon solvent using a global optimization method. The potential models of the $Ba^{2+}Ar$ and Ar-Ar interactions are well explained in our previous work [19]. The barium is a heavy and pollutant metal [20-22] and it has been used for environmental goals and in stellar [23-31]. The geometric structures, as well as the physicochemical properties of Ba2+Arn clusters with n=1–25, have never been investigated, both theoretically and experimentally. Therefore, we have compared our results with those obtained for similar systems, particularly $Mg^{m+}Ar_n$ with n=1–18, reported in Ref. [32]. In this reference, ab-initio calculations predict that the most stable $Mg^{m+}Ar_n$ correspond to (n=3–14). In addition, we have compared our $Ba^{2+}Ar_n$ structures with those obtained by our group Gaied et al. [33] for $Ca^{2+}Ar_n$. The present paper is organized as follows: After a brief introduction, we present in section 2 an overview of the computational methods used; Section 3 is dedicated to discussing of obtained results. Comparison with similar clusters has also been made in the same section. Concluding remarks are summarized in the last section.

2. Computational methods

2.1. Potential energy model

The stabilities of the two-dimensional or three-dimensional molecular structures are mainly governed by the intra-molecular interactions. The research of stable conformations of a molecule consists of determining the minima of the total interaction's energy. Such energy can be calculated using a long and expensive quantum or a semi-empirical method. In order to facilitate the calculations, it is mainly assumed that the variable term of this energy depends on the construction of the molecule and the arrangement of its atoms: it is the principle of the empirical methods. The potential energy is composed of independent additive terms. Each term of them is represented by an analytical function including empirical parameters. Indeed, it is significant to notice that a force can describe correctly the molecular vibration spectra and it is unsuitable for describing the molecular structures. A challenge in the study and comprehension of the molecular geometries is to describe and to simulate their structural and energy properties. This problem consists in choosing analytical potentials that represent the coordinate atoms. These functions must be simple, to calculate quickly, and sufficiently specifies in an acceptable way the structural properties of the macromolecules. Forces to be considered include the intra-molecular interactions between dependent-atoms and not dependent-atoms. The interactions between dependent-atoms correspond to our ab-initio calculation for different geometries. The interactions between not dependent-atoms are represented by the Van der Waals energy model. Then, the total potential energy of $Ba^{2+}Ar_n$ systems is described by the following relation:

$$V(R) = \sum_{i=1}^{n} V_{Ba^{2+}Ar_i} + \sum_{i=1}^{n}\sum_{i<j} V_{Ar_i - Ar_j} \quad (1)$$

The first term corresponds to the interactions between the Ba^{2+} ion and the neighboring argon atoms. This closed-shell interaction is taken from the experiment work of G. K. Koyanagi et al. [34]. The authors studied the formation of the $Ba^{2+}Ar$ molecule in helium bath gas at room temperature in a selected ion flow tube tandem mass spectrometer. The Ba^{2+} was produced by electrospray ionization. Then, we have interpolated the potential energy curve of the $Ba^{2+}Ar$ molecule given by this reference using the analytical form of Tang and Tonnies as expressed in the following:

$$V_{Ba^{2+}Ar}(r) = a\exp(-br) - \frac{C_4\alpha_{Ar}}{r^4} - \frac{C_6}{r^6} - \frac{C_8}{r^8} - \frac{C_{10}}{r^{10}} \quad (2)$$

The polarizability α_{Ar} and the parameters *a*, *b*, C_4, C_6, C_8 and C_{10} of $V_{Ba^{2+}Ar}(r)$ analytical potential are regrouped in **Table 1**. The second term in Equation (2) describes the interactions argon atoms; we have used the analytical potential form of Lennard-Jones:

$$V_{Ar-Ar}(R_{ij}) = 4\varepsilon\left[\left(\frac{\sigma}{R_{ij}}\right)^{12} - \left(\frac{\sigma}{R_{ij}}\right)^{6}\right] \quad (3)$$

Where $2^{1/6}\sigma$ and ε represent respectively the equilibrium distance and the well depth of the Ar-Ar interaction. Values of ε and σ are 0.0004535 a.u. and 6.328053 a.u., respectively.

2-2 Global optimization method

We note that Monte Carlo method makes possible to obtain the absolute minimum by exploring the potential energy surface. It authorizes the system to cross potential barriers and consequently to pass from a potential well

to another. This method is used mainly in the case of small clusters. In the present work, we employed the basin-hopping method of Wales and Doye [35]. The algorithm adopted is efficient to locate global minima [35-36]. This algorithm transforms the potential energy surface $E(X)$ into a new form $E'(X) = \min_l \{E(X)\}$ by an energy minimization with respect to nuclear coordinates (X). Thereafter, the converted potential surface $E'(X)$ is explored using the Monte Carlo sampling. For each size n, 10^4 cycles were performed, and "random" displacements of all atoms were carried out. The temperature in the basin-hopping simulation was set to 200 K.

Table 1: Constants describing the experimental potential of $Ba^{2+}Ar$ interpolated using the analytical form of Tang and Tonnies.

a	b	α_{Ar}	C_4	C_6	C_8	C_{10}
245.077	1.49612	11.08	0.520065	1260.82	34546.1	-414383

3. Results and discussion

The molecular modeling associated makes possible to interpret physicochemical phenomena, to suggest new experiments. The behavior of the molecules can be simulated in a static or dynamic way. The objective of this modeling is to envisage the structure and the reactivity of the molecules. Under the molecular term of modeling, one finds various techniques of visualization and of calculation of the molecular structures. Schematically, we distinguish the techniques from molecular graphics allowing to handle it (rotation, translation, change of conformation, superposition, etc.) in an interactive way (at least on the sufficiently powerful graphic stations) and to analyze it (geometrical calculations of parameters such as distances, accessible angles, surfaces, etc). These structures can be obtained by construction starting from elements (atoms, groupings…). To pass from the initial model to the final model, it is necessary to reach several stages of optimization calling upon various techniques of calculation of molecular mechanics and/or molecular dynamics. These techniques thus constitute the second shutter of molecular modeling. They rest on the use of various methods permitting to make calculations of energy, optimizations, and simulations of molecular structures. No experimental and theoretical are available for the $Ba^{2+}Ar_n$ clusters with n=1–25. Then, we compared our data with those obtained for similar systems found by Fanourgakis and Farantos for $Mg^{m+}Ar_n$ [32]. In addition, we have compared our $Ba^{2+}Ar_n$ structures with those obtained by Gaied et al. [33] for $Ca^{2+}Ar_n$. The stable structures obtained for $Ba^{2+}Ar_n$ clusters (n =1-25) are shown in **Figure 1(a** and **b)**. In **Table 2** we tabulate the total energies *(-E),* the energy per argon atom *(-E/n)* and energy per atom *(-E/n+1).* We start our study by analyzing the geometries of these clusters. The minimum energy and equilibrium distance of the $Ba^{2+}Ar$ molecule are 9.01003 kcal/mol and 6.0 a.u, respectively. These values are compared to those founded by G. K. Koyanagi et al. (D_e= 9.01 kcal/mol and R_e= 6.0 a.u) [34]. The comparison reveals a good agreement, which confirms the accuracy of our theoretical method. For $Ba^{2+}Ar_2$, a bent form (C_{2V}) is obtained. For n=3, a pyramidal (C_{3v}) geometry has been found with the Ba^{2+} ion in the summit. The $Ba^{2+}Ar_4$ have (C_{4v}) structure; two triangular pyramids which share a common side. For n=5, the stable structure has been formed with one more argon atom in the middle of a triangle constructed by Ba^{2+} ion and two argon atoms. A very stable cluster has been detected for $Ba^{2+}Ar_8$: a square antiprism (*SA*) structure has been formed with (D_{4d}) high symmetry. The (*SA*) is very stable structure with all argon atoms being located at 6 a.u. from the barium ion. Capping this (*SA*) structure, the stable $Ba^{2+}Ar_9$ cluster is obtained with (C_{4v}) symmetry. The $Ba^{2+}Ar_{10}$ system has a structure with two crowns; the first is formed by five argon atoms while the second includes four argon atoms. The $Ba^{2+}Ar_{11}$ cluster has been obtained by adding one argon atom on the other cubic side of the $Ba^{2+}Ar_{10}$ system. This icosahedron-capped square antiprism structure with Ba^{2+} ion lies between a square and a pentagonal ring.

For n=12, regular icosahedra have been formed with (I_h) high symmetry. The twelve argon atoms complete the first solvation shell around Ba^{2+}. The icosahedron packing is predicted to be the geometrical model for the $Ba^{2+}Ar_n$ clusters. We observe that larger clusters (n>12) are formed by filling the second shell and the added argon atoms occupy sites on the exterior of the $Ba^{2+}Ar_{12}$ icosahedron. The familiar double, triple and quadruple icosahedrons structures appear at $Ba^{2+}Ar_{18}$, $Ba^{2+}Ar_{22}$ and $Ba^{2+}Ar_{25}$, respectively. Based on **Figure 1(a** and **b)**. and the above analysis, we may conclude that the mechanism of cluster forming for the $Ba^{2+}Ar_n$ clusters follows the solvated ion core model. As we have seen in **Table2**, the total energy of these clusters increases with the increase of the number of argon atoms, which explained by the increase of the repulsive interaction between electrons and argon atoms. The binding energy per argon atoms shows various regimes: increases up to n = 9,

decreases for n=10 and 11, increases again for n = 12 and decrease from n = 13. This appearance is explained by the symmetry of these clusters. The peaks for n=9 and 12 are interpreted by (D_{3h}) and (I_h) high symmetries.

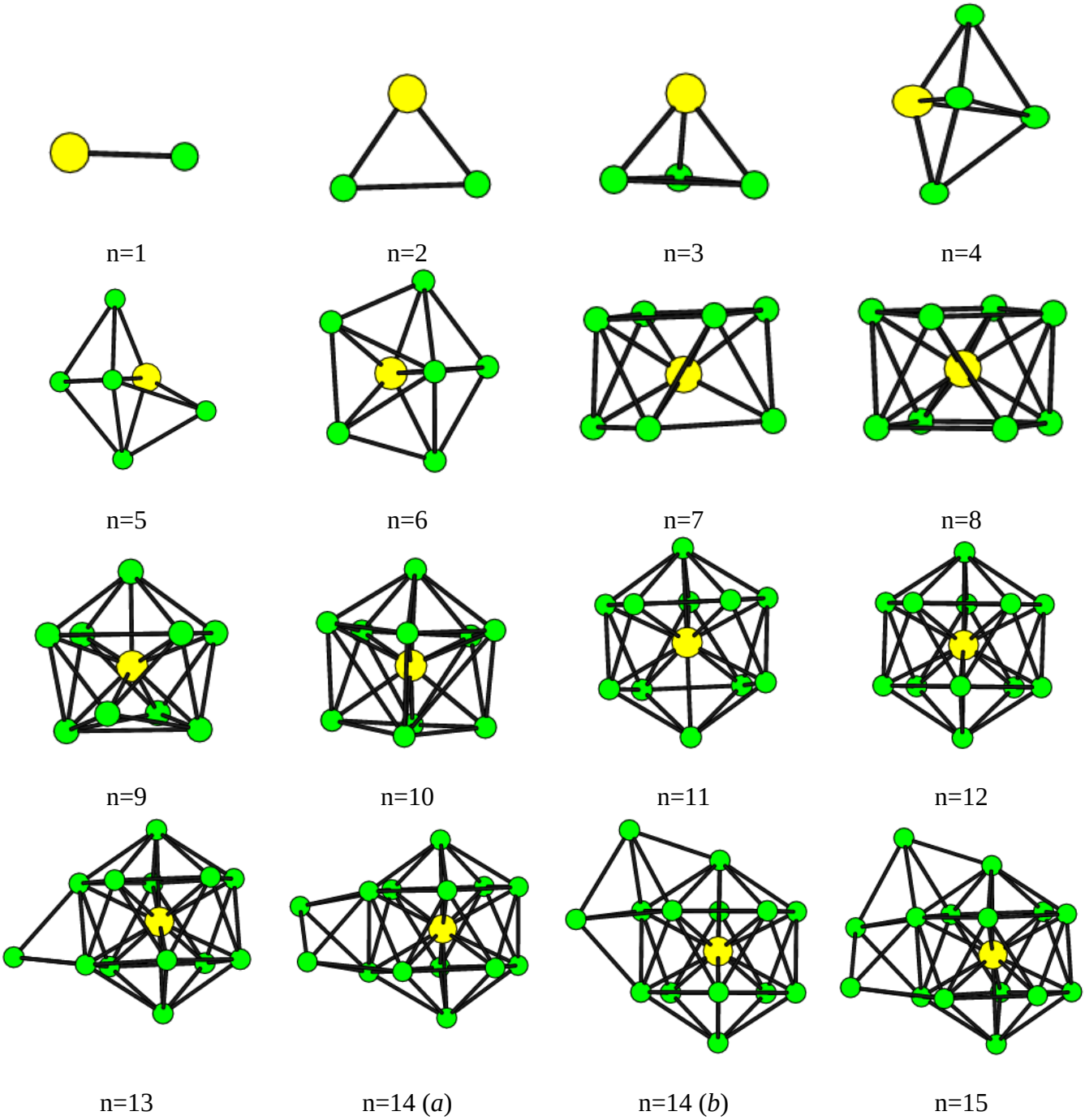

Figure 1.a: Lowest-energy isomers of $Ba^{2+}Ar_n$ clusters for sizes n=1-15.

Also, in the present study, we have interested to determine locals minima on the potential surface. The molecular mechanics treats the molecule like a whole of atoms controlled by a series of potential functions, as illustrated by the chemical binding energy. It tries to reproduce the potential energy surface corresponding to the motions of all atoms in a molecule. The first stage of calculation in molecular mechanics is to determine the inter-atomic distances and the corresponding geometries. Indeed, almost all the methods of minimization have a joint point: starting at a given place of the hyper-surface energy's coordinates, they can only determine the nearest local minimum.

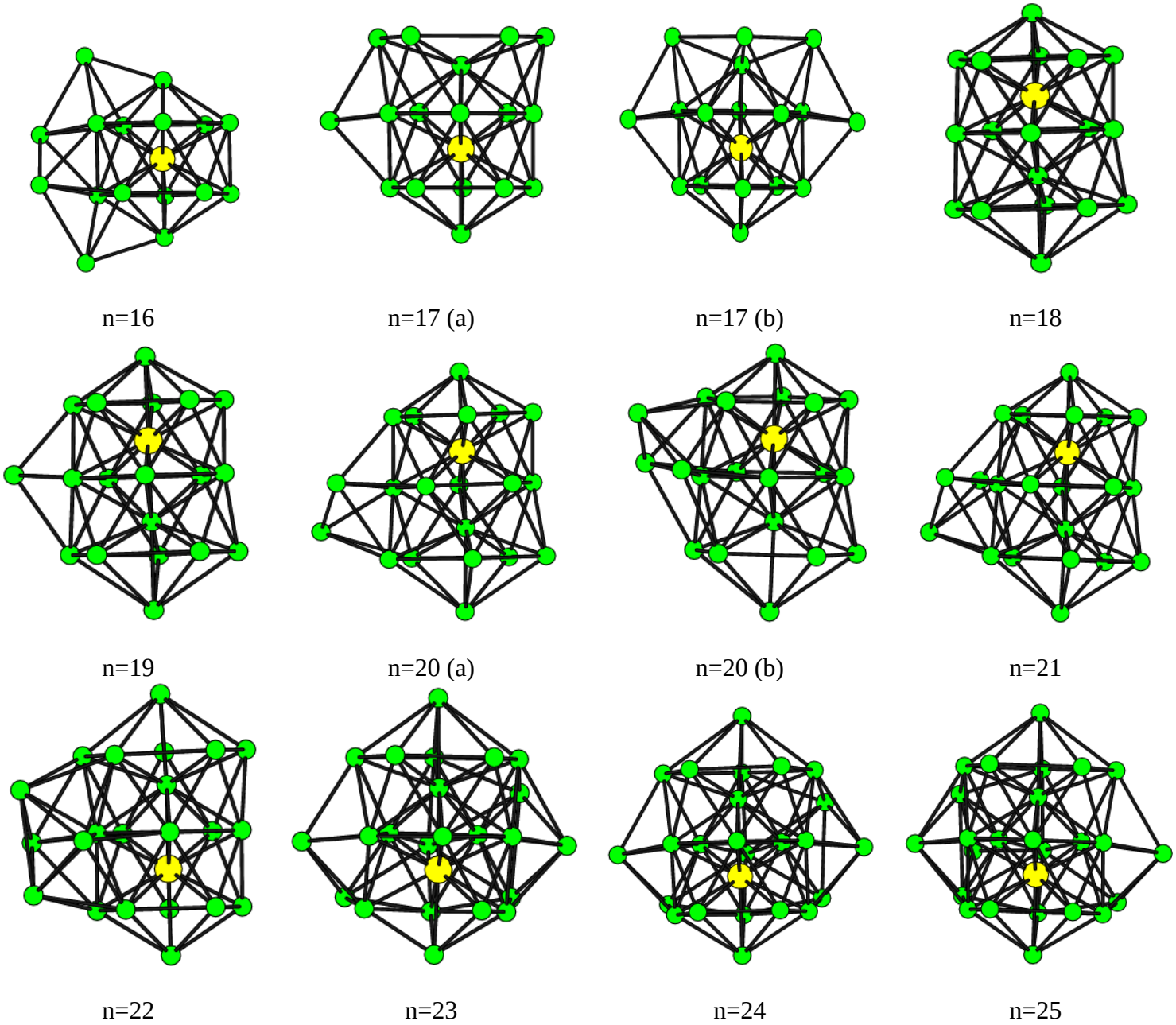

Figure 1.b: Lowest-energy isomers of $Ba^{2+}Ar_n$ clusters for sizes n=16-25.

The stability of the three-dimensional structure of a molecule is determined by the intra-molecular interactions and the interactions with the external medium. The research of stable conformations of a molecule consists of determining the minima of the total energy of interaction. To facilitate calculations, it is generally considered that the variable term of this energy depends on the construction of the molecule and the arrangement of its atoms: it is the principle of the empirical methods (mechanical molecular, dynamic molecular). The interactions between the atoms constitutive of the molecule are only taken into account. The search for a conformation then consists in making a minimization of intermolecular energy.

In this context, we find the same structure for several configurations is stable. The most important structure in our study is the most stable one. This found isomer shows that interaction between different atoms may lead to the different possible location of these atoms. These isomers are found in the following systems 14, 17 and 20. The local minima which correspond to these clusters are denoted with the letter (*b*) while the global minima with the letter (*a*). The energy differences between the two isomers (*a*) and (*b*) are small as can be seen in **Table 2**. Therefore, we can make a conclusion that this difference increased with the clusters size. For $Ba^{2+}Ar_{20}$, the difference between (*a*) and (*b*) geometries is clearly observed. The (*a*) structure is formed by adding two argon

atoms at adjacent triangular face to the double icosahedrons geometry for n=18. Thus, the (*a*) structure with high (C_{2v}) symmetry is more stable than the (*b*) one with (C_1) symmetry.

Table 2: Total energies (*-E*), energy per argon atom (*-E/n*), energy per atom (*-E/n+1*) (energies are in kcal/mol) and point groups of lowest-energy isomers of $Ba^{2+}Ar_n$ clusters (n=1-25).

n	*-E*	*-E/n*	*-E/n+1*	Point group
1	9.01003	9.01003	4.505015	$D_{\infty h}$
2	18.12826	9.06413	6.04275	C_{2v}
3	27.61926	9.20642	6.90481	C_{3v}
4	37.14708	9.28677	7.42942	C_{2v}
5	46.73066	9.34613	7.78844	C_s
6	56.44125	9.40687	8.06304	C_{3v}
7	66.20488	9.45784	8.27561	C_{3v}
8	76.31052	9.53881	8.47895	D_{4d}
9	86.31945	9.59105	8.63195	D_{3h}
10	95.18145	9.51815	8.65286	C_{3v}
11	102.42188	9.31108	8.53516	C_s
12	111.87913	9.32326	8.60609	I_h
13	113.78722	8.75286	8.12766	C_{3v}
14. a	115.9929	8.28521	7.73286	C_{2v}
14. b	115.9928	8.28521	7.73286	C_1
15	118.21288	7.88086	7.38831	C_s
16	120.4332	7.52708	7.08431	C_s
17. a	122.66072	7.21534	6.81448	C_{5v}
17. b	122.63952	7.21409	6.81331	C_s
18	124.96403	6.94245	6.57705	C_s
19	127.19548	6.6945	6.35977	C_s
20. a	129.15645	6.45782	6.15031	C_{2v}
20. b	128.91769	6,44588	6.13894	C_1
21	131.34244	6,2544	5.97011	C_1
22	133.94773	6.08853	5.82381	C_{3v}
23	136.38187	5.92965	5.68258	C_1
24	138.56767	5.77365	5.54271	C_{2v}
25	139.84152	5.59366	5.37852	C_s

Some clusters are more available than others it depends on the atom's number. These numbers are referred to as magic numbers. The magic number tells us about the most stable geometries. So the theoretical study aimed to determine the stability of configuration and explain the magic numbers. These numbers correspond to packed spheres structures. So, the stability of $Ba^{2+}Ar_n$ depends on the geometric close-packing of atoms.
The difference between the energy of the complex and the energy of the complex minus the energy of the complex featuring (*n-1*) argon atoms is calculated using the relation:

$$\Delta_1 E = E(n-1) - E(n) \quad (4)$$

Thus, the first energy difference is reported in **Figure 2** estimates the cost to add another argon atom to a complex. We have also calculated the second energy difference between size (*n*) and its immediate neighbors (*n+1*) and (*n-1*) using the relation:

$$\Delta_2 E = E(n+1) - 2E(n) + E(n-1) \quad (5)$$

The variations of $\Delta_2 E$ with (*n*) are presented in **Figure 3**. The (*n*) values with positive $\Delta_2 E$ second energy value indicate the most stable structures and form the magic number series. In this context, we have found magic $Ba^{2+}Ar_n$ clusters at n=8, 9, 10, 12, 18, 19, 22 and 23. Moreover, the geometry of resulting structures is

analyzed, and it was found that in every case, the metallic ion is situated inside the cluster. In our best knowledge, there is no experimental or theoretical existing data for our system.

The hard sphere model can be used to understand the geometric conformation of our clusters. The clusters are stable only when the distance $R_{Ba^{2+}Ar}$ between barium and argon and the distance $R_{Ar\text{-}Ar}$ between two argon atoms have the following relation:

$$d^* = R_{Ba^{2+}Ar} / R_{Ar-Ar} \leq \frac{1}{2}\left\{\left(2+\cos\frac{\pi}{k}-\cos\frac{2\pi}{k}\right)\Big/\left(1-\cos\frac{2\pi}{k}\right)\right\}^{1/2} \quad (6)$$

Using this equation, we can predict the size ratio for stability. Concerning the $Ba^{2+}Ar_n$ (n=1-25) clusters, we obtained two regular polyhedra for n=8 and n= 12. Only the icosahedron structure has a closed shell. Using this model, the most stable conformations are for n= 8, 9, 10, 12, 18, 19, 22 and 23.

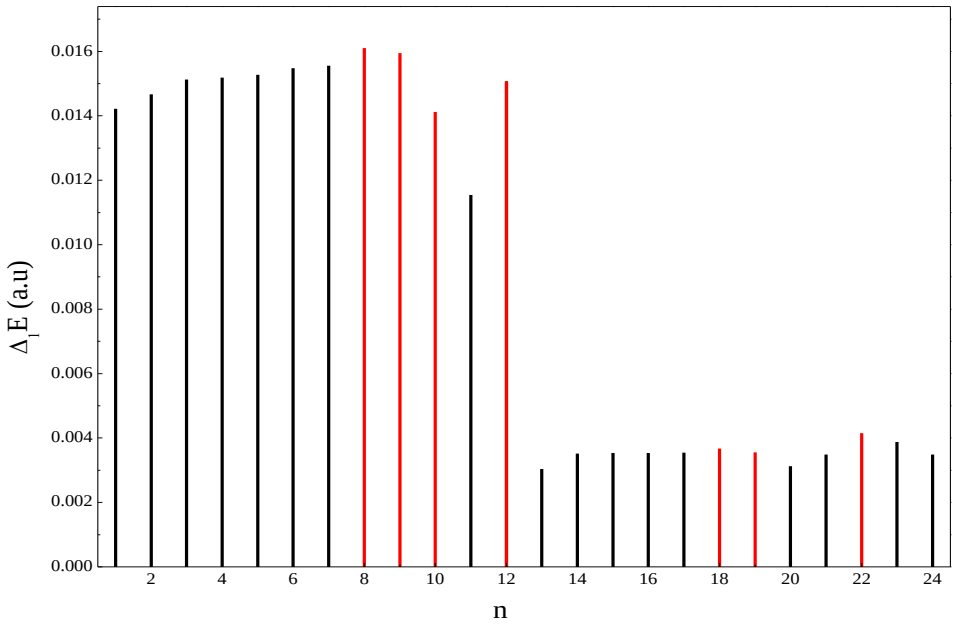

Figure 2: The energy difference Δ_1 E= E(n-1)-E(n) versus size n.

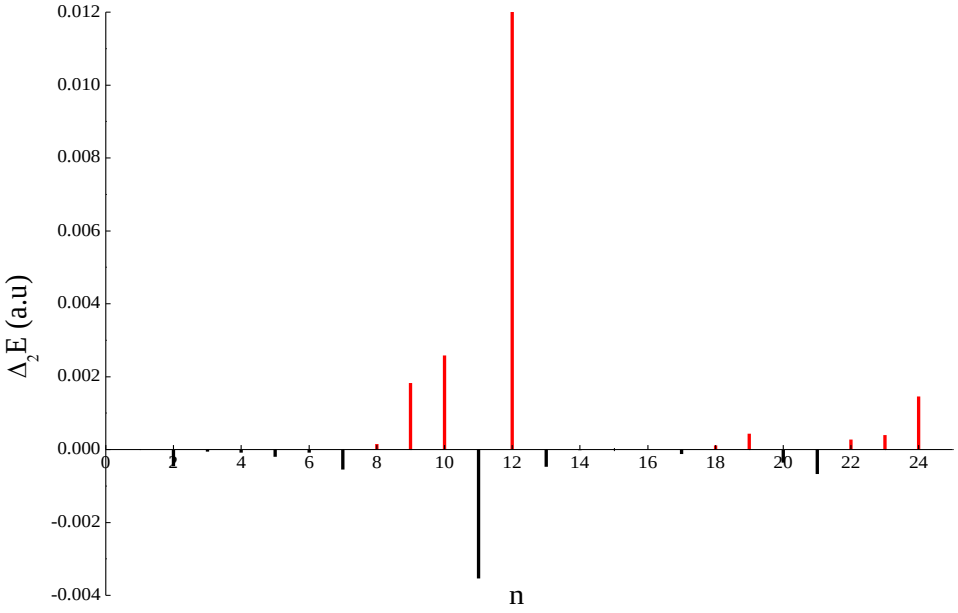

Figure 3: Second energy difference Δ_2 E= E(n+1)-2E(n)+E(n-1) versus size n.

The change of the cluster structure with the number of the atoms has a great interest. The icosahedral symmetry of argon clusters has been shown experimentally [37] and theoretically [38-40]. It was clear that the high symmetry of icosahedral packing is reflected in the stability of the clusters. The stability of MX_n clusters (M=metal ion, X=noble gas atom) has a great importance [41-49]. For the Mg^+Ar_n [43] the structure is icosahedral like pure noble gas clusters. That is, the metal ion replaces a noble gas atom in the cluster. In the previous study reported in ref. [50] some doped noble gas systems including In^+X_n , Al^+X_n and Na^+X_n (X=Ar,Kr,Xe) exhibiting the magic numbers n+1=9,11,17,21,24,26 ,27,30,..., due to capped square antiprism packing. Theoretical calculations [51-54] however, indicate that the icosahedral structure is not always the most favorable one for such clusters. Depending on the relative sizes (radii) of the ion to noble gas atoms, other structures can be more probable. The difference of size between barium, calcium and magnesium may explain the difference between the results of the cluster with argon atoms.

Therefore, our optimized geometries can be compared with those obtained for similar systems, particularly $Ba^{2+}Xe_n$ with n=1–54, reported by K. Abdessalem et al. [55]. In this previous work, the structures and stabilities of $Ba^{2+}Xe_n$ clusters ($n\leq 54$) were investigated theoretically using basin hopping global optimization method. The first solvation shell is completed as the icosahedron at n = 12, and above this size, additional xenon atoms begin to form a second layer. Then, all global minima for $Ba^{2+}Ar_n$ clusters for n equal to 2 to 25 are in concordance with the data obtained by K. Abdessalem et al. [55] for $Ba^{2+}Xe_n$ clusters.

To describe the interactions between all the atoms constituting $Ba^{2+}Ar_n$ system we have used two main hypotheses. First we assume that the charge is localized on the metal ion, and ignore charge transfer effects. It is justified by the fact that the ionization potential of the metal atom is much lower than that of the noble gas atoms and thus charge transfer is very limited. Second, we assume that only two body terms are significant in the interactions between the constituent atoms in the cluster so that the total potential energy is simply the sum of all pair potentials. It is based on the spherical character of the electronic configurations orbital of metal atom and the noble gas atoms, which is consistent with an isotropic potential. For the $Ba^{2+}Ar_n$ system, there are two main physical attractive forces to take into account. The first force is inductive, which usually exists if one of the interacting partners. The second force arises from the dispersive Van der Waals interactions. Both inductive and dispersive interactions lead to many higher order terms in the interaction potential. Magic numbers correspond to the stable cluster ions. For Ar_n clusters, hard sphere packing schemes have been examined to explain the magic numbers. These later correspond to icosahedral sequence, where an icosahedron of 12 atoms around a central atom is then surrounded by additional complete icosahedral shells. For the Ar_n clusters with n up to 25, the magic numbers are for n= 13, 19 and 23. While magic numbers for our systems occur at n+1= 9, 10, 11, 13, 19, 20, 23 and 24. The argon atoms follow geometries that can decrease the Ar / Ar distances while respecting the main lowering of energy. Consequently, the Ar / Ar interaction is a decisive factor in the formation of stable geometries

Conclusion

In the present paper, the structures and stabilities of $Ba^{2+}Ar_n$ clusters have been studied for n up to n=25. The $Ba^{2+}Ar$ interaction potential is performed by fitting the recent experimental data of G. K. Koyanagi et al. [34]. While the Ar-Ar interaction is described using the Lennard-Jones potential model. The stable geometries of the $Ba^{2+}Ar_n$ aggregates have been computed using the basin-hopping method. A square antiprism (*SA*) structure has been detected for $Ba^{2+}Ar_8$. The $Ba^{2+}Ar_{11}$ cluster has an icosahedron-capped square antiprism structure with Ba^{2+} ion lies between a square and a pentagonal ring. For n=12, a regular icosahedron has been formed. The twelve argon atoms complete the first solvation shell around Ba^{2+}. The icosahedron packing is predicted to be the core for the $Ba^{2+}Ar_n$ clusters. Then, we have obtained the double, triple and quadruple icosahedrons structures at $Ba^{2+}Ar_{18}$, $Ba^{2+}Ar_{22}$ and $Ba^{2+}Ar_{25}$, respectively. The magic numbers are determined by computing the second energy difference $\Delta_2 E$. The (n) values with positive $\Delta_2 E$ correspond to stable clusters and formed the series of magic number. In this context, we have detected "magic" clusters at n=8, 9, 10, 12, 18, 19, 22 and 23. The geometric structures of $Ba^{2+}Ar_n$ clusters with n=1–25 have never been investigated, both theoretically and experimentally. Therefore, we have compared our results with those obtained for similar systems, particularly $Mg^{2+}Ar_n$ (n=1–18) reported in Ref. [32] and $Ca^{2+}Ar_n$ (n=1–24) performed by Gaied et al [33]. The structures of the studied clusters are based on capped square antiprism (*CSA*) geometry. The difference of size between barium, calcium and magnesium may explain the difference between the results of the cluster with argon atoms. This work could be extended by taking into account the many-body effects on the structures and stabilities of $Ba^{2+}Ar_n$ (n=1–25) molecules.

References

1. Duncan M.A., Advances in Metal and Semiconductor Clusters 1, Spectroscopy and Dynamics, Elsevier, Amsterdam, ISBN: 155938171X (1993).
2. Duncan M.A., Advances in Metal and Semiconductor Clusters 2, Cluster Reaction, Elsevier, Amsterdam, ISBN: 1559387041 (1994).
3. Duncan M.A., Advances in Metal and Semiconductor Clusters 3, Spectroscopy and Structure, Elsevier, Amsterdam, (1994).
4. Haberland H., Clusters of Atoms and Molecules I, II, Springer- Verlag, Berlin, (1995)
5. Plowright R. J., McDonnell T. J., Wright T. G. and Plane J. M. C., *J. Phys. Chem. A.* 113 (2009) 9354.
6. Plowright R. J., Wright T. G. and Plane J. M. C., *J. Phys. Chem. A*, 112 (2008) 6550.
7. Kumpf R. A. and Dougherty D. A., *Science*, 261 (1993) 1708.
8. Andres R.P., Averback R.S., Brown W. L., Brus L. E., Goddard W. A., Kaldor A., Louie S. G., Moscovits M., Peercy P. S., Riley S. J., Siegel R. W., Spaepen F. and Wang Y., *J. Mater. Res.* 4 (1989) 704
9. Duncan M. A., *Annu. Rev. Phys. Chem.* 48 (1997) 69.
10. Stienkemeier, F. et Lehmann, K. *Journal of physics b-atomic molecular and optical physics* 127 (2004)
11. Toennies J. et Vilesov, A. Superuid helium droplets: *Angewandte Chemie-international*: 2622 (2006).
12. Lehnig R. et Slenczka, A. *The Journal of Chemical Physics*. 244317 (2005)
13. Grebenev S., Hartmann, M., Lindinger, A. et al. *Physica B: Condensed Matter*. 280 (2000) 65-72
14. Close J.D., Federmann, F., Ho_mann, K. et al. Helium Droplets. *Journal of Low Temperature Physics* 661 (1998).
15. Lugovoj E., Toennies, J.P. et Vilesov, A. *The Journal of Chemical Physics*: (2006) 8217.
16. Barranco M., Guardiola, R., Hernandez, S. et al. *Journal of Low Temperature Physics*: 1 (1999).
17. Dribinski V., Barbera, J., Martin, J.P. et al. Time-resolved study of solvent induced in photodissociated *IBr*-(*CO*)*n* clusters (2006) 133405.
18. Apkarian V.A. et Schwentner, N. Chemical Reviews 99, (1999) 1481,S. Chellam, P. Kulkarni, and M. P. Fraser, J. Air Waste Manage. *Assoc*.55 (2005) 60.
19. Issa K., Issaoui N., Ghalla H., Yaghmour S. J., Mahros A., Oujia B., *Mol. Phys* 114 (2016) 118.
20. Vallelonga P., and al, Earth Planet. *Sci. Lett*. 211 (2003) 329.
21. Jimi S. I., and al, Anal. Bioanal. *Chem*. 390 (2008) 495.
22. Ol'shevskii V. L.; Shchukina, N. G.; Vasil'eva, I. E. NLTE *Solar Physics*., 24 (2008) 198.
23. Mashonkina L.; Zhao, G.; Gehren, T.; Aoki, W.; Bergemann, M.; Noguchi, K.; Shi, J.
24. Takada-Hidai R., Zhang M.;, H. W. *A&A.* 478 (2008) 529.
25. Mashonkina L.; Gehren T.; Bikmaev I., *A&A.*, 343 (1999) 519.
26. Antipova L.I.; Boyarchuk A.A.; Pakhomov, Yu.V.; Panchuk, V.E. *Astronomy Reports*. 48 (2004) 597.
27. Holweger H.; Mueller, E. A. *Solar Physics.* 39 (1974) 19.
28. Barklem P. S.; Belyaev, A. K.; Spielfiedel, A.; Guitou, M.; Feautrier. N . *A&A*, 541 (2012) art. no. A80.
29. Mashonkina L.; and Zhao, G. *Astron. and Astrophys*. 456 (2006) 313.
30. Mashonkina L.; Gehren, T.; Travaglio, C.; Borkova, T.. *Astron. and Astrophys*., 397 (2003) 275.
31. Anders E.; Grevesse, N. *Geochimica et Cosmochimica. Acta*., 53 (1989) 197.
32. Fanourgakis G.S., Farantos S.C., *J. Phys. Chem*. 100 (1996) 3900.
33. Gaied W., Ben el Hadj Rhouma M. *Int. J. Quant. Chem*. 111 (2011) 652.
34. Koyanagi G. K. and Bohme D. K. J. *Phys. Chem. Lett*. 1 (2010) 41.
35. Wales, D. J.; Doyle, J. P. K. *J Phys Chem A*, 101 (1997) 5111.
36. Wales, D. J.; Scheraga, H. *Science*, 285 (1999) 1368.
37. Farges J., deFeraudy M. F., Raoult B., and Torchet G., *J. Chem. Phys*. 78 (1983) 5067.
38. Farges J., deFeraudy M. F., Raoult B., and Torchet G., *Surf. Sci*. 156 (1985) 370.
39. Harris I. A., Norman K. A., Mulkern R. V., and Northby J. A., *Chem. Phys. Lett*. 130 (1986) 316.
40. Northby J. A., *J. Chem. Phys*. 87 (1987) 6166.
41. Whetten R. L., Schriver K. E., Persson J. L., and Hahn M. Y., *J. Chem. Soc. Faraday Trans*. 86 (1990) 2375.
42. Ganteför G., Siekmann H. R., Lutz H. O., Meiwes-Broer K. H., *Chem. Phys. Lett*. 165 (1990) 293.
43. Velegrakis M. and Lüder Ch., *Chem. Phys. Lett*. 223 (1994) 139.
44. Lüder Ch., Georgiou E., and Velegrakis M., *Int. J. Mass Spectrom. Ion* Processes 153 (1996) 129.

45. Lüder Ch. and Velegrakis M., *J. Chem. Phys*. 105 (1996) 2167.
46. Vaidyanathan G., Coolbaugh M. T., Peifer W. R., and Garvey J. F., *J.Phys. Chem*. 95 (1991) 4193.
47. Desai S. R., Feigerle C. S., and Miller J. C., *J. Chem. Phys*. 97 (1992) 1793.
48. Winkel J. F., Woodward C. A., Jones A. B., and Stace A. J., *J. Chem. Phys*. 103 (1995) 5177.
49. Fanourgakis G. S. and Farantos S. C., *J. Phys. Chem.* 100 (1996) 3900.
50. Issaoui N., Abdessalem K., Ghalla H., Yaghmour S. J., Calvo F., Oujia B., *J. Chem. Phys.* 141 (2014) 174316.
51. Lüder Ch., Prekas D., and Velegrakis M., *Laser Chem.* 17 (1997) 109.
52. Perera L. and Amar F. G., *J. Chem. Phys.* 93 (1990) 4884.
53. Chartrand D. J., Shelley J. C., and LeRoy R. J., *J. Phys. Chem.* 95 (1991) 8310.
54. Wang Q., Iniquez M. P., and Alonso J. A., Z. *Phys. D* 31, (1994) 299.
55. Abdessalem K., Habli H., Ghalla H., Yaghmour S. J., Calvo F. and Oujia B., *J. Phys. Chem*. 141 (2014) 154308.

(2016) ; http://www.jmaterenvironsci.com/